Talanta 259 (2023) 124550

Contents lists available at ScienceDirect

Talanta

journal homepage: www.elsevier.com/locate/talanta

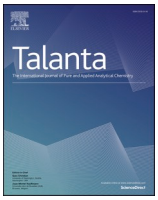

From multi to single-particle analysis: A seasonal spectroscopic study of airborne particulate matter in Zaragoza, Spain

César Marina-Montes *, Elisa Abás, Juan Buil-García, Jesús Anzano

Laser Lab, Chemistry & Environment Group, Department of Analytical Chemistry, Faculty of Sciences, University of Zaragoza. Pedro Cerbuna 12, 50009, Zaragoza, Spain

ARTICLE INFO

Keywords:
Air pollution
FESEM-EDS
ICP-MS
LIBS
PM_{10}
Raman Spectroscopy

ABSTRACT

It is distinguished that deficient outdoor air quality is responsible for substantial health and climate issues. The aim of our study was to investigate the air quality in the city of Zaragoza (Spain) by characterizing atmospheric particulate matter (PM_{10}) during two seasons (winter and spring). PM_{10} samples were collected in 2022 in quartz filters through a low-volume sampler and chemically analysed by complementary analytical techniques: Inductively Coupled Plasma-Mass Spectrometry (ICP-MS), Laser Induced Breakdown Spectroscopy (LIBS), Raman Spectroscopy (RS) and Field Emission Scanning Electron Microscopy with Energy-Dispersive X-ray Spectroscopy (FESEM-EDS). Results have revealed, together with a temperature inversion phenomenon in winter, the presence of both natural (Al, Ca, Mg, Ti, Sr, Fe, etc.) and anthropogenic particles. The latter mainly formed by black carbon with an origin on fossil fuel combustion emissions. Additionally, chemical analyses of PM_{10} filters showed the presence of three types of microplastics suspended in the air of the city: polyethylene terephthalate (PET), polyamides (PA) and polystyrene (PS). The results obtained from this research are of special interest to take into account for future air quality policies, particularly those with the aim of reducing air pollution in cities.

1. Introduction

Air pollution is known as one of our era's greatest hazards, having adversely impacts on both, human health and climate. Aerosols, a complex mixture of fine solid particles and liquid droplets suspended in the atmosphere, are part of this serious environmental concern. For this reason, there is a growing interest by the scientific community in the study of atmospheric aerosols. Analyzing the composition of aerosol particulate matter (PM) is fundamental when investigating its impact and sources [1], particularly PM with an aerodynamic diameter of 10 μm or less (PM_{10}). For instance, it is known that PM_{10} pollution is linked to increase rates of mortality due to cardiovascular and respiratory illnesses [2,3].

Considering the negative effects of PM on health, PM_{10} concentration is currently legislated in the European Union by the directive 2008/50/CE. Based on an annual and on a 24-h average, the directive limits PM_{10} concentration to 28 $\mu g/m^3$ and 35 $\mu g/m^3$, respectively. The latter PM_{10} concentration should not be exceeded more than 35 times in any calendar year [4]. Additionally, the WHO (World Health Organization) has its own global air quality guidelines [5].

The chemical composition of ambient PM_{10} depends on different aspects: source of PM_{10}, season of the year and weather conditions [6–8]. Regarding the source, natural sources include species originated from the earth's crust, whereas anthropogenic sources include PM derived from human activities. Besides, aerosols can be distinguished between primary or secondary, where secondary aerosols are formed by transformation mechanisms from primary gaseous emissions. Nowadays, most people live in cities close to industrial parks [9]. In urban areas, road traffic is considered one of the main sources of PM_{10} [10]. Nevertheless, additional human sources exist, such as industry, residential heating and shipping emissions [11,12]. Among anthropogenic elements, As, Pb, Cd, Hg, Zn, Ni, Cu, and Cr are interesting due to their toxic character, while others, such as Al, Fe, Ca, Ti, and Li are mainly linked to the resuspension of soil (earth's crust) [13]. As previously commented, PM_{10} chemical composition can also be altered by the season of the year [14]. This fact is coherent with the different human activities conducted during the entire year. For example, since heating and traffic activities are greater in winter, some studies evidence higher PM_{10} concentration values on this season [15].

Taking into account the small size and weight of aerosol particles, the meteorology of a specific region, along with the source and season of the year, plays a crucial role in the nature of atmospheric aerosols [16].

* Corresponding author.
E-mail address: cesarmarinamontes@unizar.es (C. Marina-Montes).

https://doi.org/10.1016/j.talanta.2023.124550
Received 1 March 2023; Received in revised form 27 March 2023; Accepted 11 April 2023
Available online 12 April 2023

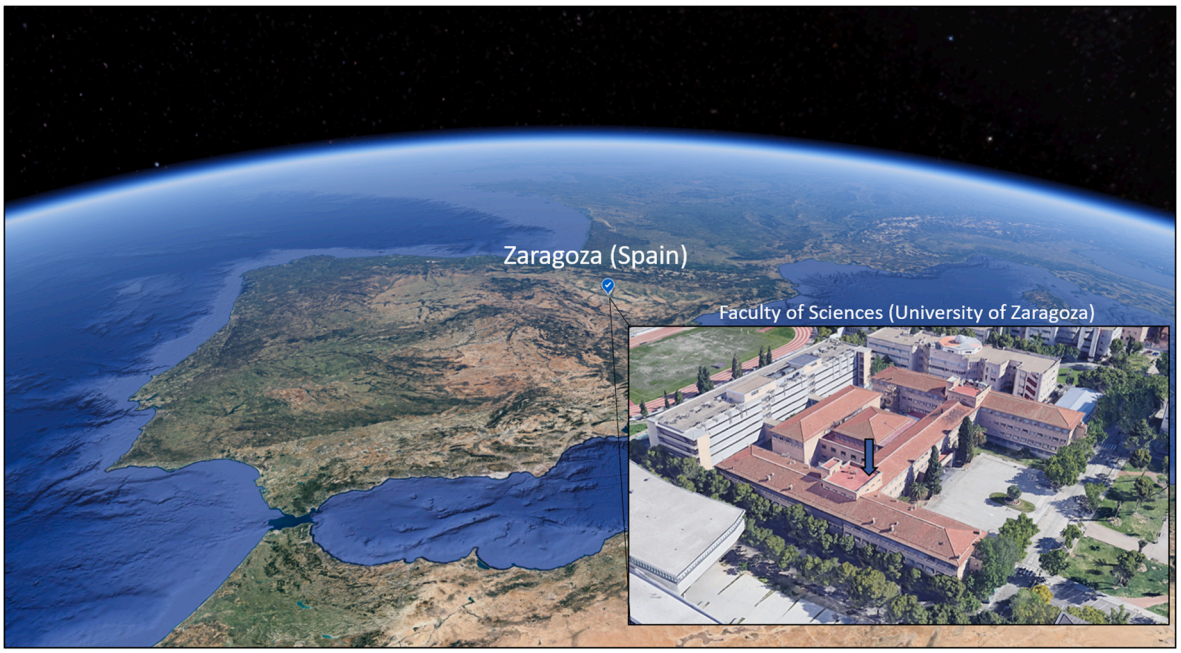

Fig. 1. Map of Spain with the location of Zaragoza. The blue arrow shows the exact position of the low volume sampler on the roof of the Faculty of Sciences (San Francisco Campus, University of Zaragoza, Spain). Images taken from Google Earth Pro.

Therefore, determined by wind patterns, PM_{10} is capable of traveling thousands of kilometers away from its original source, remaining suspended in the troposphere from hours to weeks [17,18]. In dry regions, such as the south of Europe, low rainfall rates facilitate the resuspension of soil particles. Thus, the crustal fraction of PM_{10} composition becomes highly relevant [19].

Environmental and health effects of PM_{10} depend on their elemental composition. Thus, a complete characterization of PM_{10} chemical composition is needed. Traditional analytical techniques for the characterization of airborne PM_{10} elemental composition are Inductively Coupled Plasma-Optical Emission Spectroscopy (ICP-OES), and/or Inductively Coupled Plasma-Mass Spectrometry (ICP-MS) [13,20]. Both techniques are distinguished by their high performance. Recently, Laser Induced Breakdown Spectroscopy (LIBS) has demonstrated its potential to study atmospheric aerosols in the air quality field [21]. LIBS allows a fast multi-elemental analysis of PM_{10} collected in filters with minimum sample destruction. Both, ICP-MS and LIBS were implemented in this study. On the other hand, individual particles are of vital importance on the composition and sources of aerosols. These particles can internally be made of various elements. In the interest of chemically characterize single particles, Raman spectroscopy (RS) and Field Emission Scanning Electron Microscopy with Energy-Dispersive X-ray Spectroscopy (FESEM-EDS) were additionally employed. RS is a rapid and no-destructive technique which allows to determine the chemical structure, morphology, etc., of individual particles. Finally, FESEM-EDS has the ability to complement Raman analysis, as well as to provide qualitative elemental analysis of the individual particles. The combination of these five power analytical techniques (ICP-MS, LIBS, RS and FESEM-EDS) allowed to accomplish a completely characterization (chemical and morphological) of PM_{10} collected on filters.

In this context, the present study aims to analyze and compare the psychochemical composition and potential sources of ambient PM_{10} sampled at two different seasons (winter and spring) in the city of Zaragoza (NW Spain). PM_{10} sources mainly include vehicles and residential heating. Furthermore, Zaragoza has a big industrial park, principally formed by automotive, metal, appliances, and textile manufacturing industries. Along with this, Zaragoza airport is considered Spain's second largest cargo airport. Thus, vehicle together with residential, industrial and plane PM_{10} emissions are expected. During these seasons, anthropogenic activities and meteorology were expected to differ. The obtained results will be a powerful tool for helping to establish additional mitigation strategies for reducing air pollution in the city of Zaragoza at a specific time.

2. Materials and methods

2.1. Study location and filter sampling

The study was performed on the strategic city of Zaragoza, located in the North-East of Spain, being Spain's fifth-largest city in terms of population (~700,000 inhabitants). The climate of Zaragoza is semi-arid Mediterranean continental with a particularly dominant, strong, and dry north-westerly wind called Cierzo.

PM_{10} samples were collected on the roof of the Faculty of Sciences (41°38′30″ N; 0°53′59″ W, San Francisco Campus, University of Zaragoza, Spain), at a height of ~40 m above street level (Fig. 1). Although the campus is closed to non-university road traffic (only student and employee parking is allowed), the site is surrounded by high traffic density roads and residential buildings.

Each PM_{10} sample was collected during winter and spring days (2022) on circular quartz filter (47 mm diameter, Pallflex) at 24-h period (from 9:00 to 9:00 h, local time), through a low volume sampler (Derenda LVS 3.1, 2.3 m^3/h). A total of 18 and 16 samples were collected from the 10th to 28th of January (winter period), and 9th to May 27, 2022 (spring period), respectively.

In order to obtain the mass concentrations of the collected samples and following the standard gravimetric measurement method (EN12341:2015) [22], PM_{10} filters were stabilized for two days in a temperature and humidity controlled chamber (20 °C, 50%) and weighted before and after sampling, in accordance with standard procedures. After determining the mass concentration of each PM_{10} filter sample, samples were selected and analysed by different reference analytical techniques: ICP-MS, LIBS, RS and FESEM-EDS.

Meteorological data for the study were obtained from the meteorological station managed by the Spanish Meteorological Agency (AEMET) located in Zaragoza airport (41°39′23″N; 0°52′45″W).

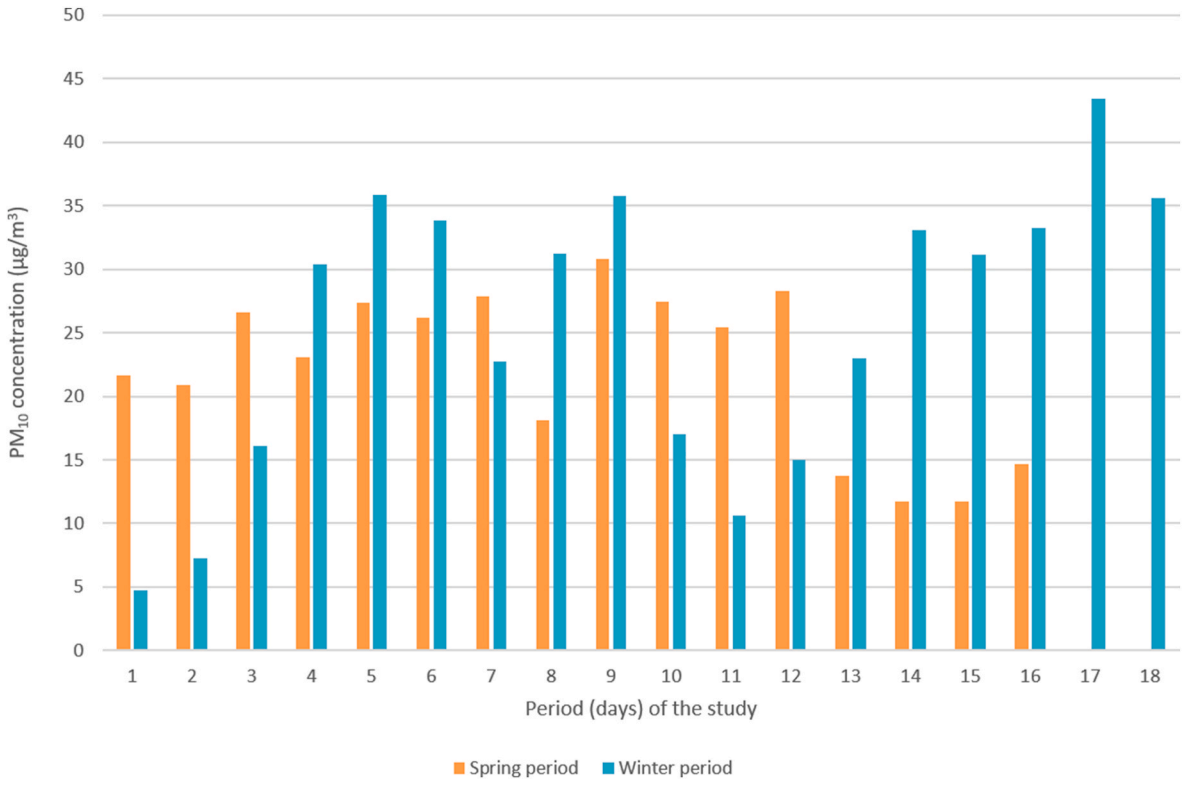

Fig. 2. Time variation of PM_{10} (µg/m^3) values in Zaragoza corresponding to the winter and spring periods of the study (2022).

2.2. Contamination prevention

With the aim of preventing contamination by external particles, meticulous and strict measures were taken during sampling manipulation and processing. Filter samples were carefully handled and stored with laboratory film in Petri dishes using tweezers, single-use nitrile globes and white cotton laboratory coat, as performed in previous works [21,23–25]. Besides, blank filters were also analysed by the different analytical techniques.

2.3. ICP-MS

PM_{10} chemical composition was determined following a protocol already published and greatly employed in the literature [26]. Half of each individual filter was cut and acid digested (2.5 mL HNO_3 at 65%: 5 mL HF at 40%: 2.5 mL $HClO_4$ at 60%) for the analysis of elements by ICP-MS (PerkinElmer Elan DRC-e). External calibration was implemented by ICP-MS using standard solutions (0.25, 0.5, 1, 2, 5 and 10 ppb and a HNO_3 5% blank).

2.4. LIBS

A Q-switched Nd:YAG laser (Brilliant Quantel, model Ultra CFR) operating at 1064 nm with a 7.7 ns pulse width, 2.6 mm diameter laser beam and a maximum pulse energy of 50 mJ, was used for LIBS PM filter analysis. PM filter samples were placed inside a special chamber (LIBS-SC, Ocean Optics) where the laser beam was directly focused on the samples through a 150 mm focal length lens. Plasma light was collected by an optical fiber (QP50-2-UV-BX, Ocean Insight) connected to an Echelle spectrometer (Andor Mechelle ME5000, 195 mm focal length, F/7, l/Al 5000) with an attached intensified charge coupled detector (Andor iStar DH734, 1024 × 1024 pixels 13.6 × 13.6 µm^2 by pixel, 18 mm of intensifier diameter). Before measuring the samples, the spectrometer and detector were calibrated using a low pressure mercury-argon lamp (HG-1, Ocean Optics). Filter measurements were accomplished under Argon atmosphere. A total of 3 spectra were obtained per sample. Each obtained spectrum was the accumulation of 10 measurements at different points of the sample. From the 3 spectra, the average spectrum of each PM_{10} filter sample was obtained. The selected pulse energy was 25 mJ, delay time 750 ns, and integration gate 1000 ns.

2.5. Raman Spectroscopy

Raman measurements on each filter were carried out by using a Raman Jasco NRS-3100 spectrometer, enclosing a microscope and a polychromator with charge coupled detector (1024 × 128 pixel). Microscope uses an automated mapping stage (XYZ) with auto-focusing option controlled by a joystick that simplifies focusing on and searching for particles of interest on the filter samples. Raman spectrum were obtained using an excitation wavelength of 532 nm (Nd:YAG laser) and the laser power was set at 1–5 mW. Acquisition parameters: 25 s and 250 accumulations.

2.6. FESEM instrumentation

A Carl Zeiss MERLIN™ Field Emission Scanning Electron Microscope with an attached energy-dispersive X-ray (EDS) analyser (Oxford Instruments) were used for investigating the chemical composition, size and shape of individual PM collected on each selected filter. Filter samples were covered by a thin layer of conductive carbon (5–10 nm) under vacuum conditions (10^{-7} mbar). The accelerating voltage was set at 5-15Kv with a magnification ranging from 70 to 40,000 x. FESEM analysis were performed by General Services Research Support (SAI) of University of Zaragoza.

2.7. Enrichment factor

The Enrichment Factor (EF) was used to study crustal or anthropogenic sources on the PM filters from the study area [20] during the

different seasons (winter and spring). The EF of each element was calculated as a normalization of the element of interest against a reference element (Ti in our case) following the equation:

$$EF = \left(A_{sample} \ / \ B_{sample}\right) / \left(A_{background} \ / \ B_{background}\right) \quad (1)$$

where, A_{sample} is the concentration of the element under study in the filters, and B_{sample} is the concentration of the reference element (Ti) in the filters. $A_{background}$ is the concentration of the same element under study in the background sample and $B_{background}$ is the concentration of the reference element (Ti) in the background sample. The composition of the upper continental crust (background sample) was obtained from Rudnick and Gao (2003) [27].

The obtained EF values for each element were divided into five levels of pollution [28]. EF < 2 indicates zero or minimal pollution; 2 ≤EF < 5 indicates moderate pollution; 5 ≤EF < 20 indicates significant pollution; 20 ≤EF < 40 indicates strong pollution and EF ≥ 40 indicates extreme pollution.

2.8. Air-mass back trajectory frequency modelling

During two seasons (winter and spring), the potential sources of PM_{10} in Zaragoza were investigated by using back trajectory frequencies obtained using the online NOAA (National Oceanic and Atmospheric Administration) HYSPLIT (Hybrid Single Particle Lagrangian Integrated Trajectory) software [29,30] and the GDAS (Global Data Assimilation System) 1-degree meteorological data. Numerous previous studies have used HYPLIT software and GDAS datasets to investigate aerosol sources in different places [20,31,32].

In winter and spring, the number of days to calculate trajectory frequencies were 18 and 19, respectively. Each 48-h backward trajectory was calculated from the study site at 6-h intervals at a height of 40 m AGL (Above Ground Level) and a resolution of 1°. The obtained data were employed to plot percentage frequency distributions.

3. Results and discussion

3.1. PM_{10} concentration

As shown in Fig. 2, PM_{10} daily concentration measured in our study ranged from 4.71 to 43.39 μg/m^3 (mean 25.56 μg/m^3) and from 11.68 to 30.79 μg/m^3 (mean 22.23 μg/m^3) during the winter and spring periods, respectively. It can be observed that three of these PM_{10} daily values in winter exceeded the limit daily value of 35 μg/m^3 established by the current air quality European Directive [4]. In relation to the mean PM_{10} concentration values, these were close to the annual mean PM_{10} concentration limit value of 28 μg/m^3 established by the European Directive and higher than the annual mean PM_{10} concentration limit value of 15 μg/m^3 recommended by the WHO global air quality guideline [5]. Additionally, compared to other Spanish urban areas, similar mean PM_{10} concentrations were reported [33]. These mean values were distant to the annual mean PM_{10} concentration value of 42.9 μg/m^3 obtained in Zaragoza in 2002 [34]. This fact implies that the current European directive on air quality [4] has achieved satisfactory results in reducing PM_{10} concentrations in cities. Notwithstanding, PM_{10} concentration values found in Zaragoza were considered high, especially in winter.

During the winter period, ten samples reached values higher than the mean PM_{10} concentration (25.56 μg/m^3). These episodes of high PM_{10} concentrations were mainly obtained due to the specific meteorological conditions associated with those days: low wind speed, with values lower than 3.3 km/h, and low temperatures. Concerning the wind speed, it noted that high wind speed contributes to the renewal of the PM_{10} suspended in the air, helping to its cleanliness and dispersing the PM_{10} over longer distances [35]. Fig. S1a in supplementary materials shows a correlation plot of the two data sets (wind speed vs PM_{10} concentration) yielding a value of $r^2 = 0.81$ (p-value <0.05). Thus, the lower wind speed, the higher PM_{10} concentration values are observed. In relation to the spring period (Fig. S1b), this correlation prevails, although it is less marked than in winter ($r^2 = 0.56$; p-value <0.05).

During the winter period, in addition to the strong dependence observed between PM_{10} concentration and wind speed, minimum daily temperatures were also correlated with an increase on PM_{10} concentration ($r^2 = 0.69$; p-value <0.05), as shown in Fig. S1c (supplementary materials). This fact is attributed to the temperature inversion phenomenon, as reported by other studies [36,37]. Temperature inversion produces a stratification in the air layers, trapping the PM_{10} in the lower layers of the atmosphere and playing a major role in air quality, especially in winter and in valleys, such as the Ebro valley where Zaragoza is located. Therefore, low temperatures (cool air), recorded during specific days of the study, favored the presence of this meteorological thermal inversion.

Table 1
Mean concentration values (ng/m^3) of some major and minor elements corresponding to the winter and spring period of the study (2022) developed in Zaragoza.

	Element	Winter	Spring
Major compounds (ng/m^3)	Ca	765.76	5656.27
	K	395.43	401.01
	Al	388.02	–
	Na	374.77	770.74
	Ti	130.85	292.37
	Mg	85.49	211.89
Minor compounds (ng/m^3)	Zn	24.99	15.29
	Cr	10.44	14.21
	Ba	7.29	6.76
	Mn	7.15	6.82
	Cu	5.96	3.77
	Sn	5.63	4.56
	Pb	4.08	1.70
	Zr	3.89	5.17
	Sr	2.15	4.31
	As	–	1.12
	Hf	0.21	0.23
	La	0.16	0.22
	Co	0.15	0.39
	Ga	0.03	0.71

3.2. Chemical analysis

As shown in Table 1, the chemical analysis (ICP-MS) of the PM_{10} filters from the city of Zaragoza showed the presence of some major elements (mean value > 50 ng/m^3) following the sequence Ca > K > Al > Na > Ti > Mg and Ca > Na > K > Ti > Mg in winter and spring period, respectively. In addition to the major elements found by ICP-MS in the PM_{10} filter samples, this technique showed the presence of some minor elements (mean value < 50 ng/m^3) following this order Zn > Cr > Ba > Mn > Cu > Sn > Pb > Zr > Sr > Hf > La > Co > Ga (winter period) and Zn > Cr > Mn > Ba > Zr > Sn > Sr > Cu > Pb > As > Ga > Co > Hf > La (spring period).

3.2.1. Major compounds

Pearson's correlation coefficients of the major elements are shown in Table S1 (supplementary materials). As seen, in winter all the major elements are significantly positively correlated. However, during the spring period this correlation remains just for some elements (Ca/K/Mg), and an additional correlation appears (Ti/Na). Similar correlations suggest a common source of elements.

EFs of major and minor elements are displayed in Fig. 3. Regarding the major elements, in both seasons Al and Mg have mean EFs lower than 2, confirming its mainly natural source. Na and K have mean EFs values between 2 and 5, which indicates moderate pollution; while Ca have mean EFs higher than 5 (Winter) and 20 (Spring), which mean

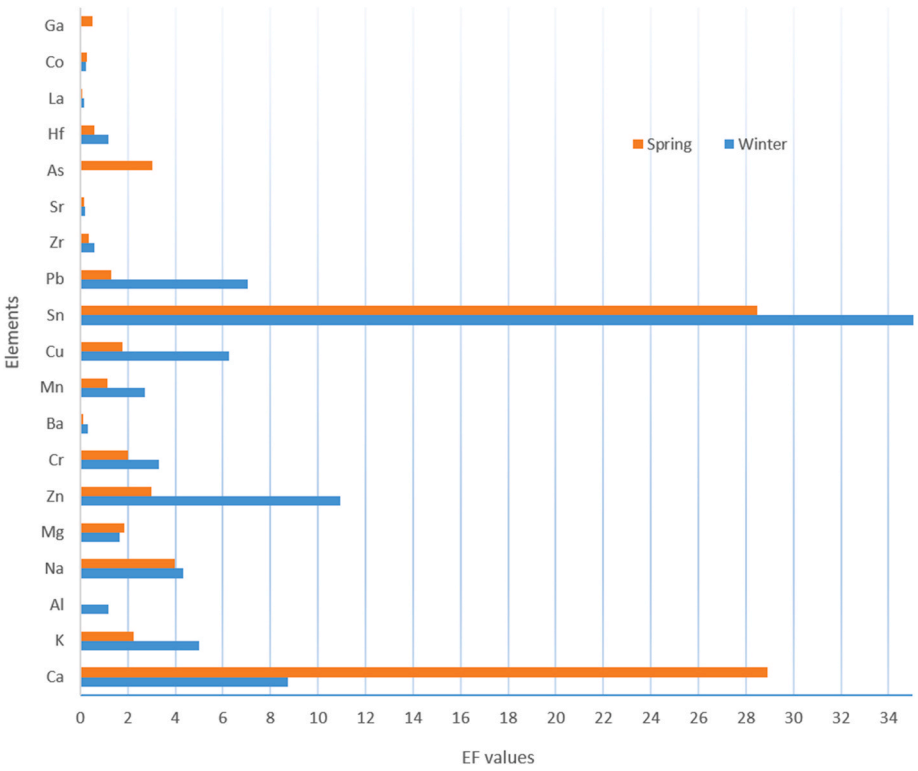

Fig. 3. Enrichment Factor (EF) values of some major and minor elements in Zaragoza corresponding to the winter and spring periods of the study (2022).

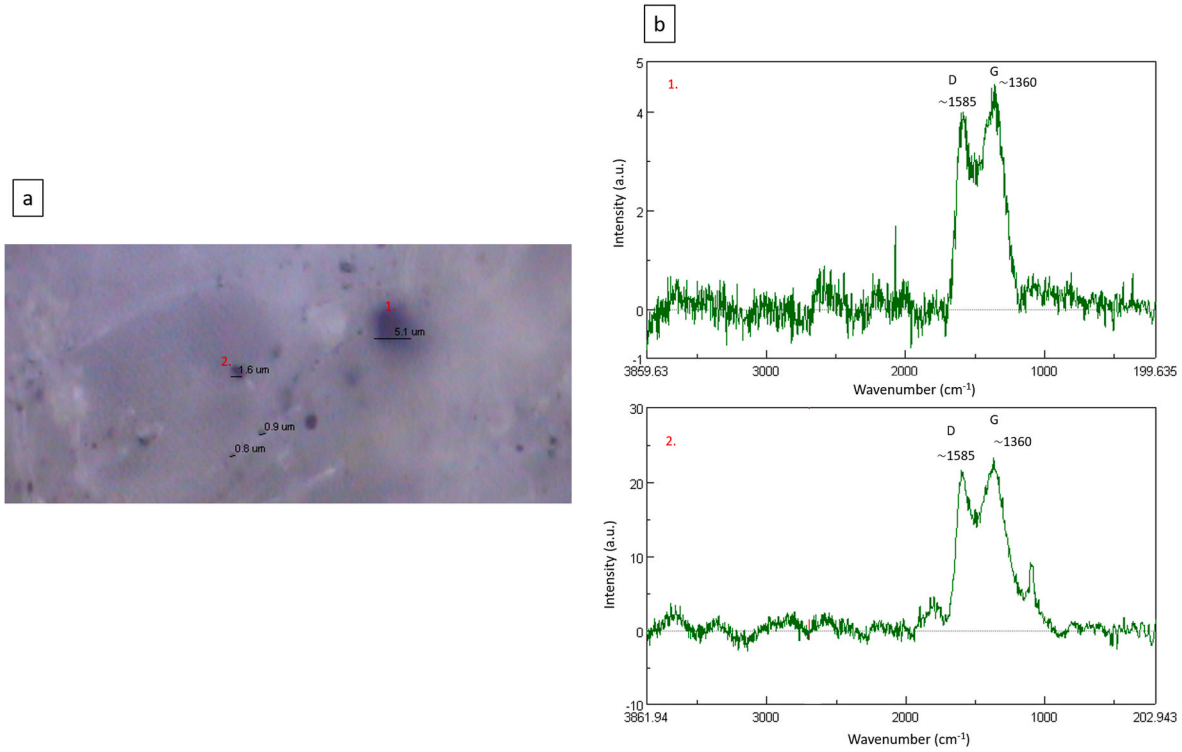

Fig. 4. Raman image (a) and spectra (b) of different BC (black carbon) particles found in one of the PM_{10} filter samples (winter).

significant and strong pollution, respectively.

Based on these results and in agreement to previous studies [13,38], the higher mean concentrations associated to Ca, Al, Ti and Mg can be attributed to soil resuspension, with an origin on the earth crust; while some other elements, such as Na and K, are associated to marine contributions (Mediterranean and/or Cantabrian sea) [34]. In addition, the high EF values associated with Ca can be explained by a relatively close building activity (renovation of the Faculty of Philosophy and Letters).

Supporting ICP-MS results, LIBS filter analysis of both seasons

showed the presence of previous major elements: Ca, K, Al, Na, Ti and Mg. Besides, LIBS technique added the identification of Fe as a major element. An averaged LIBS winter spectrum is presented in Fig. S2, where the most intense signals, shown in Table S2, were used for the elemental identification. Due to the silicic nature of the filters, blank filter spectra showed intense signals of Si and O. Additionally, blank filters revealed a few and low intensity lines of Ca and Na.

An interesting element to investigate because its general importance in climate and health is black carbon (BC). BC is considered of the main pollutants in the atmosphere and is produced by the incomplete combustion of fossil fuels [39]. BC contains elemental carbon and some hydrogen and oxygen. In a city like Zaragoza, BC sources are mainly residential heating, industrial activities and vehicular traffic. Raman measurements confirmed the presence of individual BC particles in the PM_{10} filters (winter and spring).

Fig. 4 shows some of these multiple BC particles found in the winter PM filters (a) with two (1 and 2) of their corresponding Raman spectra (b). This Raman spectrum includes the two characteristic overlapping bands of carbon at ~1360 cm^{-1} and ~1585 cm^{-1}, as described in the literature [24,40,41]. Depending on the type of carbon, these bands can differ from wavenumbers and forms. The first band corresponds to the D band, while the second band corresponds to the G band. The ratio of the D to G peaks indicates the relative amount of edge to volume of the crystals [40]. The G peak corresponds to the E_{2g} mode of bulk crystalline graphite. On the other hand, the D peak is induced by the breakdown of graphite near the crystal edges. As seen in Fig. S3 (supplementary materials), the intensity ratio (I_D/I_G) of different BC particles (a-f) found in the PM filters was in the range 0.86–1.22. This ratio range is in agreement with previous studies [24,41], where carbon particles were associated to diesel and gasoline emissions (residential heating, industrial activities and vehicular traffic). Based on Raman results, the number of individual BC particles was considerably reduced in the spring filters. This indicates that the main winter source of BC particles in Zaragoza is residential heating (diesel emissions).

FESEM-EDS filter analysis added morphological information on each individual particle, combined with its elemental composition. These analyses confirmed the presence and composition of multiple BC particles on different winter PM filters as well as added some other particles rich in Na, Mg, Al, Ca, P, S, Cs, Cu and Fe (Fig. S4). The elements detected distinct to C were mostly related to the presence of iron, aluminum and copper oxides with an origin on soil resuspension during both periods (Figs. S4b and S5a). Of course, in the spring period, different types of pollen and vegetal particles were found (Figs. S5b and c).

3.2.2. Minor compounds

According to Pearson's correlation coefficients of minor elements (Table S1), in winter all minor elements, except Pb, Sn and Ga, are significantly positively correlated. Additionally, these minor elements are significantly correlated with the previous major elements from winter, suggesting a common origin. On the other hand, during the spring period it can be clearly observed two groups of elements positively correlated. The first group (Zn/Mn/Cu/Co) is correlated with the main group of major elements (Ca/K/Mg), while the second group (As/Cr/Ba/Zr/Sn/Hf/Ga) is correlated with Na and Ti. Additionally, Sn (winter) and Pb (spring) reflect additional sources, based on their lack of correlation with previous elements.

As seen in Fig. 3, in both seasons Ba, Zr, Sr, Hf, La, Co, and Ga have mean EF values lower than 2, which confirm their natural source. Based on the winter period, Cr, Mn and As, with their EF values between 2 and 5, are categorized as moderately contaminated; while Pb, Zn and Cu, with their EF values between 5 and 20, are defined as significantly contaminated. The presence of Cr, Mn, As and Pb in PM_{10} filter samples is usually related to industrial activities, primarily produced in metallurgical processes (copper and steel production) [13]. Concerning Zn and Cu, these elements are typically related to road traffic emissions,

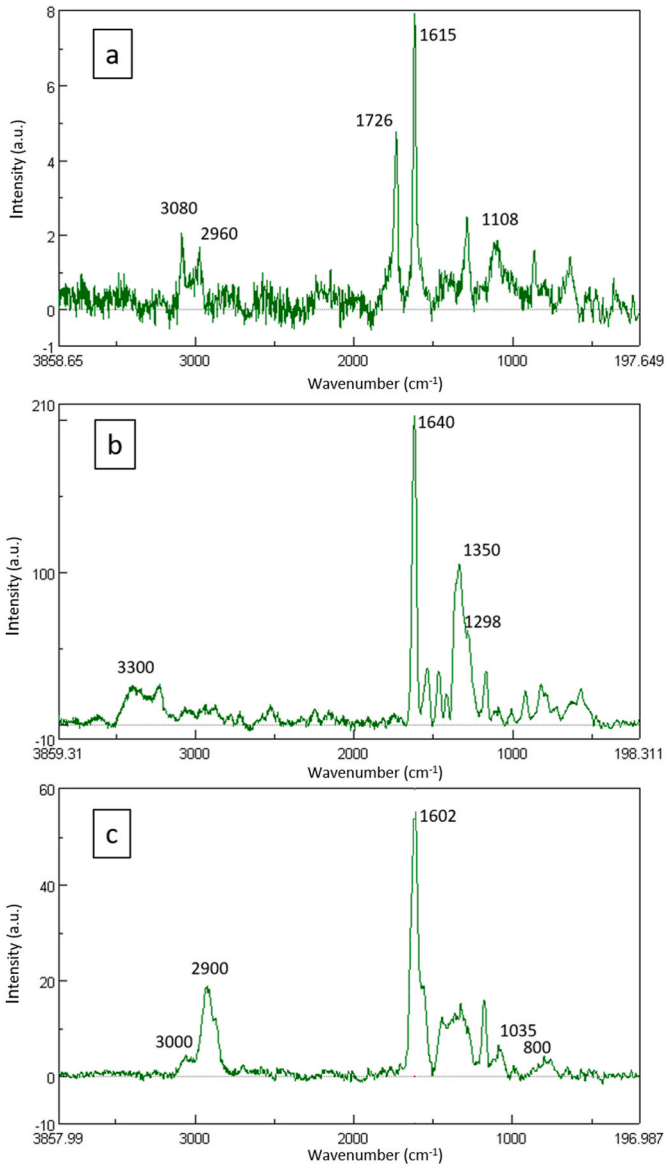

Fig. 5. Raman spectra of three different microplastic fibers made of polyethylene terephthalate (PET) (a), polyamide (PA) (b) and polystyrene (PS) (c) found in winter (2022).

linked to tyre and brake abrasion [13]. Both elements were also identified by LIBS measurements in some of the filters. On the other hand, during the spring period the EF values of Cr, Mn, Pb and Cu were 2.03, 1.16, 1.31 and 1.77, respectively. These values were lower or close to 2, reflecting the lack of contamination of these elements in Spring. Finally, the maximum EF values correspond to Sn, indicating extreme (winter) and strong (spring) pollution of this element, predominantly linked to road traffic and steel industry [13,38,42].

In general, EF values for most of the elements were higher in winter. This can be explained by the previously reported temperature inversion phenomena, together with a higher consumption of residential heating and vehicles [15,43]. Overall, based on Pearson correlation coefficients, combined with EF values, elements in our study can be classified into three categories: predominantly crustal (Ca, Al, Ti, Mg, Ba, Zr, Sr, Hf, La, Co and Ga), marine (K and Na), mixed (Cr, Mn, As, Pb, Zn and Cu) and anthropogenic (Sn).

Along with the previous amorphous carbon species found by RS and FESEM-EDS, a single graphite particle was also identified in one of the winter PM filters. The big difference between amorphous carbon and

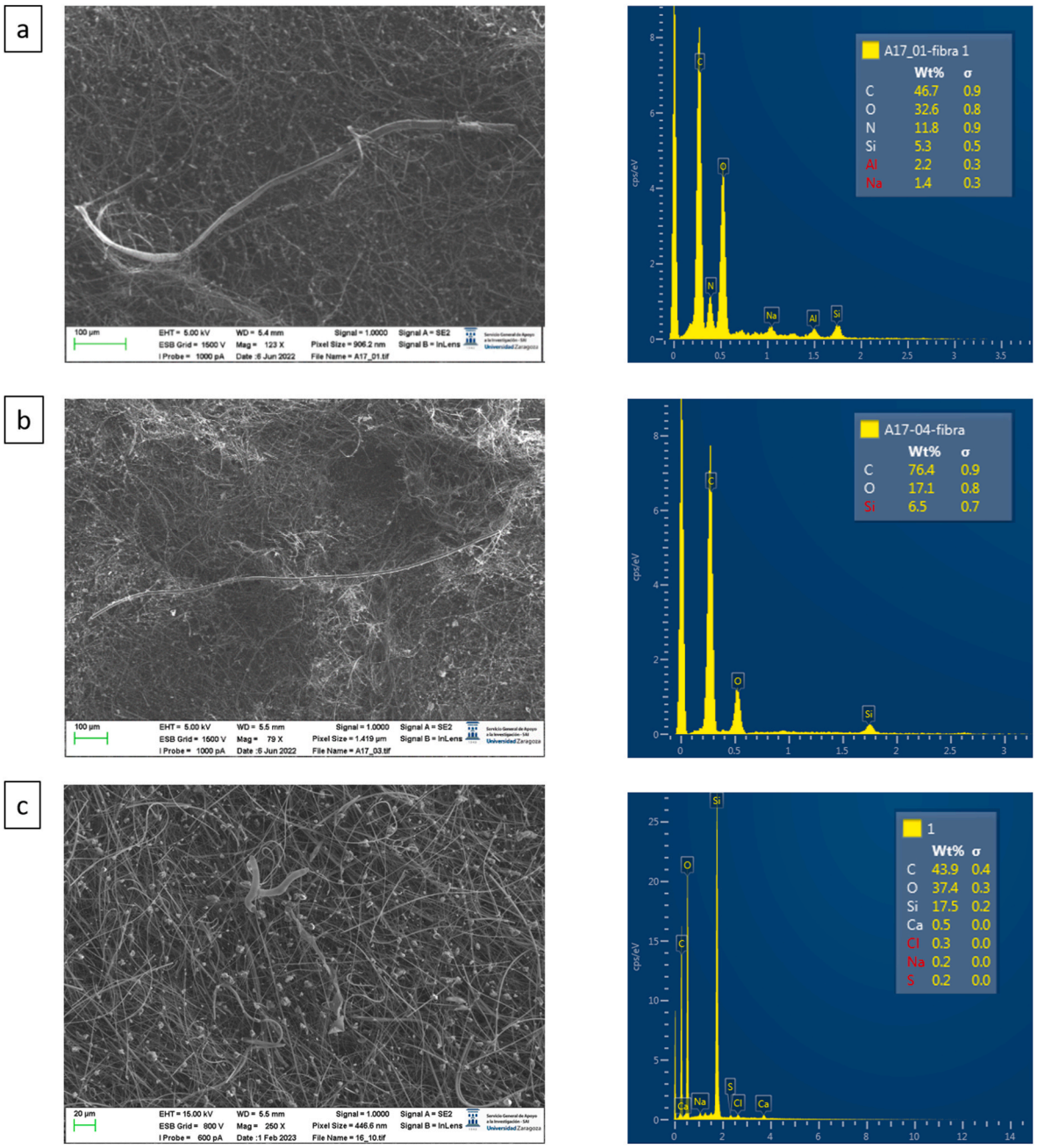

Fig. 6. SEM images and EDX spectra for three MP samples. (a) PA fiber (winter) together with additional PM material: Al and Na., (b) PET fiber (winter), and (c) PET fiber (spring) with additional material: Ca, Cl, Na and S. In all samples, Si has an origin on the silicic nature of the filter material.

graphite is that the latter is characterized by an ordered internal structure, crystallizing in the hexagonal system, forming parallel layers where each carbon atom has sp2 hybridization [44]. Raman spectrum of a graphite particle with its hexagonal structure image is shown in Fig. S6 (supplementary materials). It exhibits defect (D) and graphitic (G) bands at ~1360 cm^{-1} and ~1585 cm^{-1}, and a 2D band at ~2720 cm^{-1} associated to the first overtone of the D1 band [45]. The detection of this particle in only one of the filters on a single filter region, reveals its likely natural origin from a relatively close (~150 km northwest of Zaragoza) quarry (Azkarate Quarry) in Esteríbar (Navarre, Spain).

Continuing with the analysis of the filters by RS, some plastics fibers were identified in two and 6 PM_{10} filters of winter and spring, respectively. Since the size of these plastic fibers was lower than 5 mm, they were considered as microplastics (MPs). The dominant MPs found in the city of Zaragoza were made of polyethylene terephthalate (PET), with its main Raman bands at 1108, 1615, 1726, 2960 and 3080 cm^{-1} (Fig. 5a), polyamides (PA), with its main Raman bands at 1298, 1350, 1640 and 3300 cm^{-1} (Fig. 5b) [46]; and polystyrene (PS), with its main Raman bands at 800, 1035, 1602, 2900, 3000 cm^{-1} (Fig. 5c) [46–48]. PA were found specially during the spring period. In some occasions, the main Raman bands of these MPs were seen together with the background bands provided by the filter. These broad bands were observed around 610, 800, 980 and 1890 cm^{-1} due to the silicic nature of the fibers composing the filter.

Repeatedly, FESEM-EDS analysis added morphological information on each individual MP fiber, combined with its elemental composition. Imaging and analysis of MPs fibers by this technique corroborated the presence of PA (Fig. 6a) and PET (Fig. 6b and c).

Similar studies have found, among others, this type of polymers (PET, PA and PS) in different cities worldwide, such as Paris (France)

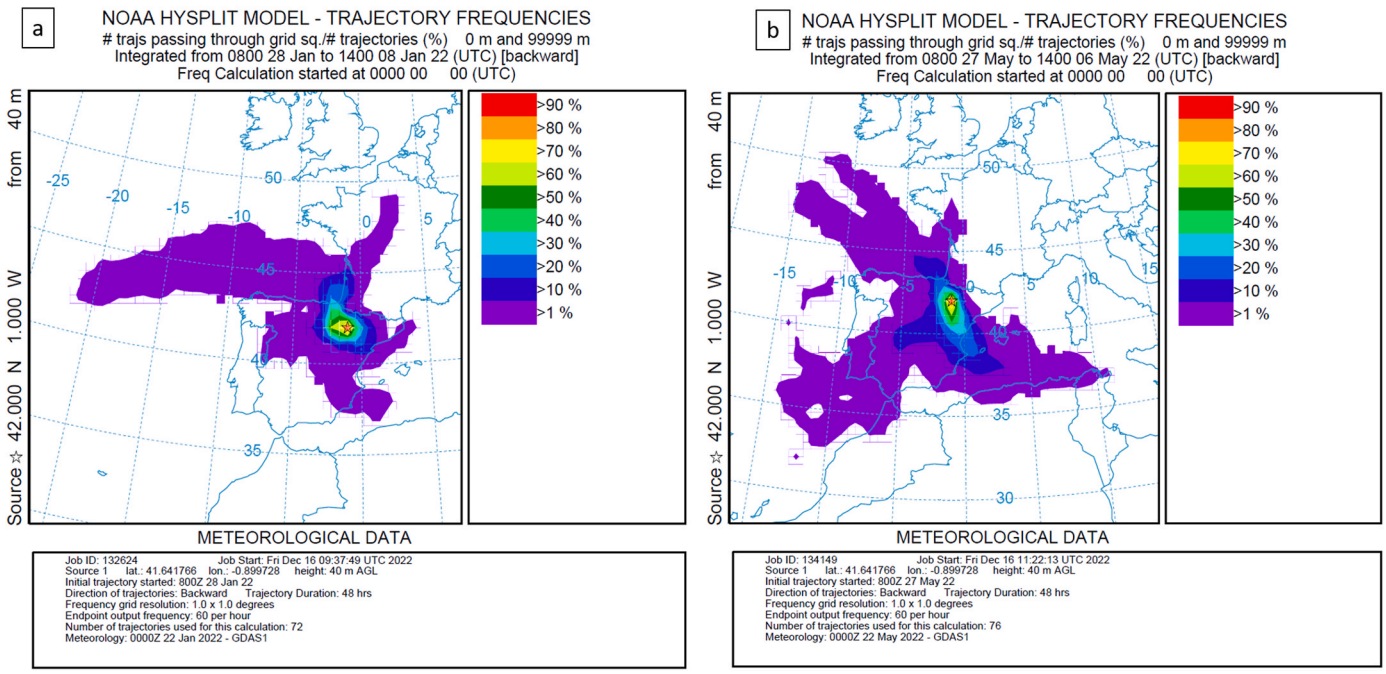

Fig. 7. Trajectory frequencies showing the number of trajectories passing through a grid. (a) Data for winter (8–January 28, 2022). (b) Data for spring (6–May 27, 2022).

[49], Yantai and Shanghai (China) [50,51], Hamburg (Germany) [52] and Ahvaz (Iran) [25]. PET is employed in recyclable goods, packaging material, and textile industry [53]; while PA is used in fishery goods, household commodities (carpets, rugs, etc.), clothes and industrial activities [54]. Finally, PS is used in packaging material and manufacturing industries [55].

Concerning MPs small size and density, MPs are able to be easily transported by air over long distances [56], reaching a wide range of locations distinct to their original source (mainly urban areas) [57]. MPs have been found in natural environments [56,58], and even in fresh water [59], snow [60] and air [24] from Antarctica. The presence of MPs on the environment has innumerable risks, causing damage to ecosystems [61], human health [62,63] and perturbing the climate [64].

3.3. Air-mass back trajectory frequency modelling

Fig. 7 shows trajectory modelling results during the winter (a) and spring (b) season in the city of Zaragoza calculated for an endpoint 40 m AGL using the GDAS1 dataset. In both seasons, frequency distribution results indicate a broad region of potential aerosol sources (land use, industries, airport, vehicles, residential heating, etc.). Besides, 70–90% frequencies are located relatively close to the study area (maximum 37 km), spreading to the west and south of Zaragoza city in winter and spring seasons, respectively. Thus, trajectory calculations confirm the previously mentioned local origin of most of the observed aerosols. The great variety of these potential natural and/or anthropogenic local sources explains the heterogeneity of the aerosols studied in Zaragoza during both seasons.

4. Conclusions

Air quality in Zaragoza, the fifth most populated city inSpain, was seasonally monitored (winter and spring) by collecting PM_{10} samples in circular fiber filters through a low volume sampler. The main goal of the study was to identify the PM_{10} psychochemical composition present in the city during the two seasons and its potential sources. Since nowadays it does not exist a unique analytical technique capable to completely characterize PM_{10} deposited in filters, psychochemical analysis of samples was determined by various complementary analytical techniques (ICP-MS, LIBS, Raman and FESEM-EDS).

The exhaustive analytical characterization of PM_{10} revealed the presence of different particles made of elements with a natural (Al, Ca, Mg, Ti, Sr, Fe, etc.), marine (K and Na), mixed (Cr, Mn, As, Pb, Zn and Cu) and anthropogenic (Sn) source. Besides, BC was found to be the dominated anthropogenic particle, especially in winter, with its origin in diesel and gasoline emissions. Finally, microplastic pollution was detected by the presence of polymer fibers made of PET, PA and PS.

This investigation improves seasonal air pollution knowledge in the city of Zaragoza and its potential sources. Therefore, additional measurements on the city aiming to tackle or reduce air pollution, together with raising public awareness on air pollution, should be considered.

Author contributions statement

César Marina-Montes: Writing-original draft, Methodology, Formal analysis. **Elisa Abás**: Writing-original draft, Methodology, Formal analysis. **Juan Buil-García**: Methodology, Formal analysis. **Jesús Anzano**: Project administration, Funding acquisition, Supervision.

All authors have read and agreed to the published version of the manuscript.

Declaration of competing interest

The authors declare that they have no known competing financial interests or personal relationships that could have appeared to influence the work reported in this paper.

Data availability

Data will be made available on request.

Acknowledgments

The authors gratefully acknowledge the University of Zaragoza for facilities and material resources and the NOAA Air Resources Laboratory (ARL) for the provision of the HYSPLIT transport and dispersion model

and/or READY website (https://www.ready.noaa.gov) used in this publication. Authors would like to acknowledge the use of Servicio General de Apoyo a la Investigación-SAI (Universidad de Zaragoza), and Servicio de Cromatografía y Espectroscopía- INMA (UNIZAR-CSIC). This project forms part of Government of Aragon proposal E23_17D and E49_20 R. CMM's work was funded through a postdoctoral contract (POP-FPI) granted by the Spanish Government (PRE2018-085309). Financial support from the European Social Fund & University of Zaragoza is acknowledged. Graphical abstract and Fig. 1 have been taken from Google Earth Pro.

Appendix A. Supplementary data

Supplementary data to this article can be found online at https://doi.org/10.1016/j.talanta.2023.124550.

References

[1] P. Heikkilä, A. Rostedt, J. Toivonen, J. Keskinen, Elemental analysis of single ambient aerosol particles using laser-induced breakdown spectroscopy, Sci. Rep. 12 (1) (2022), 14657.
[2] F. Oduber, A. Castro, A.I. Calvo, C. Blanco-Alegre, E. Alonso-Blanco, P. Belmonte, R. Fraile, Summer-autumn air pollution in León, Spain: changes in aerosol size distribution and expected effects on the respiratory tract, Air Qual. Atmos. Health 11 (5) (2018) 505–520.
[3] K.-H. Kim, E. Kabir, S. Kabir, A review on the human health impact of airborne particulate matter, Environ. Int. 74 (2015) 136–143.
[4] Eu-Parlament, The European parliament and the council of the European union "directive 2008/50/EC of 21 may 2008 on ambient air quality and cleaner air for Europe, OJ L 152 (2008) 1–44.
[5] O. World Health, WHO Global Air Quality Guidelines: Particulate Matter (PM2.5 and PM10), Ozone, Nitrogen Dioxide, Sulfur Dioxide and Carbon Monoxide, World Health Organization, Geneva, 2021.
[6] M. Hallquist, J.C. Wenger, U. Baltensperger, Y. Rudich, D. Simpson, M. Claeys, J. Dommen, N.M. Donahue, C. George, A.H. Goldstein, J.F. Hamilton, H. Herrmann, T. Hoffmann, Y. Iinuma, M. Jang, M.E. Jenkin, J.L. Jimenez, A. Kiendler-Scharr, W. Maenhaut, G. McFiggans, T.F. Mentel, A. Monod, A.S. H. Prévôt, J.H. Seinfeld, J.D. Surratt, R. Szmigielski, J. Wildt, The formation, properties and impact of secondary organic aerosol: current and emerging issues, Atmos. Chem. Phys. 9 (14) (2009) 5155–5236.
[7] S.M.L. Hama, R.L. Cordell, J. Staelens, D. Mooibroek, P.S. Monks, Chemical composition and source identification of PM10 in five North Western European cities, Atmos. Res. 214 (2018) 135–149.
[8] M. Röösli, G. Theis, N. Künzli, J. Staehelin, P. Mathys, L. Oglesby, M. Camenzind, C. Braun-Fahrländer, Temporal and spatial variation of the chemical composition of PM10 at urban and rural sites in the Basel area, Switzerland, Atmos. Environ. 35 (21) (2001) 3701–3713.
[9] M. Millán-Martínez, D. Sánchez-Rodas, A.M. Sánchez de la Campa, A. Alastuey, X. Querol, J.D. de la Rosa, Source contribution and origin of PM10 and arsenic in a complex industrial region (Huelva, SW Spain), Environ. Pollut. 274 (2021), 116268.
[10] Y. González-Castanedo, D. Sanchez-Rodas, A.M. Sánchez de la Campa, M. Pandolfi, A. Alastuey, V.E. Cachorro, X. Querol, J.D. de la Rosa, Arsenic species in atmospheric particulate matter as tracer of the air quality of Doñana Natural Park (SW Spain), Chemosphere 119 (2015) 1296–1303.
[11] S. Philip, R.V. Martin, G. Snider, C.L. Weagle, A. van Donkelaar, M. Brauer, D. K. Henze, Z. Klimont, C. Venkataraman, S.K. Guttikunda, Q. Zhang, Anthropogenic fugitive, combustion and industrial dust is a significant, underrepresented fine particulate matter source in global atmospheric models, Environ. Res. Lett. 12 (4) (2017), 044018.
[12] Z. Klimont, K. Kupiainen, C. Heyes, P. Purohit, J. Cofala, P. Rafaj, J. Borken-Kleefeld, W. Schöpp, Global anthropogenic emissions of particulate matter including black carbon, Atmos. Chem. Phys. 17 (14) (2017) 8681–8723.
[13] X. Querol, M. Viana, A. Alastuey, F. Amato, T. Moreno, S. Castillo, J. Pey, J. de la Rosa, A. Sánchez de la Campa, B. Artíñano, P. Salvador, S. García Dos Santos, R. Fernández-Patier, S. Moreno-Grau, L. Negral, M.C. Minguillón, E. Monfort, J. I. Gil, A. Inza, L.A. Ortega, J.M. Santamaría, J. Zabalza, Source origin of trace elements in PM from regional background, urban and industrial sites of Spain, Atmos. Environ. 41 (34) (2007) 7219–7231.
[14] S. Sobanska, G. Falgayrac, J. Rimetz-Planchon, E. Perdrix, C. Brémard, J. Barbillat, Resolving the internal structure of individual atmospheric aerosol particle by the combination of Atomic Force Microscopy, ESEM–EDX, Raman and ToF–SIMS imaging, Microchem. J. 114 (2014) 89–98.
[15] M. Viana, W. Maenhaut, X. Chi, X. Querol, A. Alastuey, Comparative chemical mass closure of fine and coarse aerosols at two sites in south and west Europe: implications for EU air pollution policies, Atmos. Environ. 41 (2) (2007) 315–326.
[16] I. Barmpadimos, C. Hueglin, J. Keller, S. Henne, A.S.H. Prévôt, Influence of meteorology on PM10 trends and variability in Switzerland from 1991 to 2008, Atmos. Chem. Phys. 11 (4) (2011) 1813–1835.
[17] J.H. Seinfeld, S.N. Pandis, Atmospheric Chemistry and Physics: from Air Pollution to Climate Change, John Wiley & Sons, Inc., Hoboken, 2006.
[18] IPCC, Climate Change 2013: the Physical Science Basis. Contribution of Working Group I to the Fifth Assessment Report of the Intergovernmental Panel on Climate Change, Cambridge University Press, Cambridge, United Kingdom and New York, NY, USA, 2013.
[19] N.T. Kim Oanh, N. Upadhyay, Y.H. Zhuang, Z.P. Hao, D.V.S. Murthy, P. Lestari, J. T. Villarin, K. Chengchua, H.X. Co, N.T. Dung, E.S. Lindgren, Particulate air pollution in six Asian cities: spatial and temporal distributions, and associated sources, Atmos. Environ. 40 (18) (2006) 3367–3380.
[20] C. Marina-Montes, L.V. Pérez-Arribas, M. Escudero, J. Anzano, J.O. Cáceres, Heavy metal transport and evolution of atmospheric aerosols in the Antarctic region, Sci. Total Environ. 721 (2020), 137702.
[21] C. Marina-Montes, V. Motto-Ros, L.V. Pérez-Arribas, J. Anzano, M. Millan-Martinez, J.O. Caceres, Aerosol analysis by micro laser-induced breakdown spectroscopy: a new protocol for particulate matter characterization in filters, Anal. Chim. Acta 1181 (2021), 338947.
[22] U.E., Standard Gravimetric Measurement Method for Determination of the PM10 or PM2.5 Mass Concentration of Suspended Particulate Matter, 2015, 12341.
[23] E. Abás, C. Marina-Montes, M. Laguna, R. Lasheras, P. Rivas, P. Peribáñez, J. del Valle, M. Escudero, A. Velásquez, J.O. Cáceres, L.V. Pérez-Arribas, J. Anzano, Evidence of human impact in Antarctic region by studying atmospheric aerosols, Chemosphere 307 (2022), 135706.
[24] C. Marina-Montes, L.V. Pérez-Arribas, J. Anzano, S.F.-O. de Vallejuelo, J. Aramendia, L. Gómez-Nubla, A. de Diego, J.M. Madariaga, J.O. Cáceres, Characterization of atmospheric aerosols in the antarctic region using Raman spectroscopy and scanning Electron microscopy, Spectrochim. Acta Mol. Biomol. Spectrosc. 266 (2022), 120452.
[25] S. Abbasi, N. Jaafarzadeh, A. Zahedi, M. Ravanbakhsh, S. Abbaszadeh, A. Turner, Microplastics in the atmosphere of Ahvaz city, Iran, J. Environ. Sci. 126 (2023) 95–102.
[26] X. Querol, A. Alastuey, S. Rodriguez, F. Plana, C.R. Ruiz, N. Cots, G. Massagué, O. Puig, PM10 and PM2.5 source apportionment in the Barcelona Metropolitan area, Catalonia, Spain, Atmos. Environ. 35 (36) (2001) 6407–6419.
[27] R.L. Rudnick, S. Gao, 3.01 - composition of the continental crust, in: H.D. Holland, K.K. Turekian (Eds.), Treatise on Geochemistry, Pergamon, Oxford, 2003, pp. 1–64.
[28] H. Yongming, D. Peixuan, C. Junji, E.S. Posmentier, Multivariate analysis of heavy metal contamination in urban dusts of Xi'an, Central China, Sci. Total Environ. 355 (1) (2006) 176–186.
[29] G. Rolph, A. Stein, B. Stunder, Real-time environmental applications and display sYstem: READY, Environ. Model. Software 95 (2017) 210–228.
[30] A.F. Stein, R.R. Draxler, G.D. Rolph, B.J.B. Stunder, M.D. Cohen, F. Ngan, NOAA's HYSPLIT atmospheric transport and dispersion modeling system, Bull. Am. Meteorol. Soc. 96 (12) (2015) 2059–2077, available at: https://www.ready.noaa.gov/HYSPLIT_traj.php.
[31] L. Su, Z. Yuan, J.C.H. Fung, A.K.H. Lau, A comparison of HYSPLIT backward trajectories generated from two GDAS datasets, Sci. Total Environ. 506–507 (2015) 527–537.
[32] S.-b. Hong, Y.J. Yoon, S. Becagli, Y. Gim, S.D. Chambers, K.-T. Park, S.-J. Park, R. Traversi, M. Severi, V. Vitale, J.-H. Kim, E. Jang, J. Crawford, A.D. Griffiths, Seasonality of Aerosol Chemical Composition at King Sejong Station (Antarctic Peninsula) in 2013, Atmospheric Environment, 2019, 117185.
[33] M. Millán-Martínez, D. Sánchez-Rodas, A.M. Sánchez de la Campa, J. de la Rosa, Contribution of anthropogenic and natural sources in PM10 during North African dust events in Southern Europe, Environ. Pollut. 290 (2021), 118065.
[34] J.M. López, M.S. Callén, R. Murillo, T. García, M.V. Navarro, M.T. de la Cruz, A. M. Mastral, Levels of selected metals in ambient air PM10 in an urban site of Zaragoza (Spain), Environ. Res. 99 (1) (2005) 58–67.
[35] R. Cichowicz, G. Wielgosiński, W. Fetter, Effect of wind speed on the level of particulate matter PM10 concentration in atmospheric air during winter season in vicinity of large combustion plant, J. Atmos. Chem. 77 (1) (2020) 35–48.
[36] P.J. Silva, E.L. Vawdrey, M. Corbett, M. Erupe, Fine particle concentrations and composition during wintertime inversions in Logan, Utah, USA, Atmos. Environ. 41 (26) (2007) 5410–5422.
[37] E. Malek, T. Davis, R.S. Martin, P.J. Silva, Meteorological and environmental aspects of one of the worst national air pollution episodes (January, 2004) in Logan, Cache Valley, Utah, USA, Atmos. Res. 79 (2) (2006) 108–122.
[38] X. Querol, A. Alastuey, M.M. Viana, S. Rodriguez, B. Artiñano, P. Salvador, S. Garcia do Santos, R. Fernandez Patier, C.R. Ruiz, J. de la Rosa, A. Sanchez de la Campa, M. Menendez, J.I. Gil, Speciation and origin of PM10 and PM2.5 in Spain, J. Aerosol Sci. 35 (9) (2004) 1151–1172.
[39] T.C. Bond, S.J. Doherty, D.W. Fahey, P.M. Forster, T. Berntsen, B.J. DeAngelo, M. G. Flanner, S. Ghan, B. Kärcher, D. Koch, S. Kinne, Y. Kondo, P.K. Quinn, M. C. Sarofim, M.G. Schultz, M. Schulz, C. Venkataraman, H. Zhang, S. Zhang, N. Bellouin, S.K. Guttikunda, P.K. Hopke, M.Z. Jacobson, J.W. Kaiser, Z. Klimont, U. Lohmann, J.P. Schwarz, D. Shindell, T. Storelvmo, S.G. Warren, C.S. Zender, Bounding the role of black carbon in the climate system: a scientific assessment, J. Geophys. Res. Atmos. 118 (11) (2013) 5380–5552.
[40] S.K. Sze, N. Siddique, J.J. Sloan, R. Escribano, Raman spectroscopic characterization of carbonaceous aerosols, Atmos. Environ. 35 (3) (2001) 561–568.
[41] Y. Feng, L. Liu, Y. Yang, Y. Deng, K. Li, H. Cheng, X. Dong, W. Li, L. Zhang, The application of Raman spectroscopy combined with multivariable analysis on source apportionment of atmospheric black carbon aerosols, Sci. Total Environ. 685 (2019) 189–196.
[42] M.C. Minguillón, X. Querol, U. Baltensperger, A.S.H. Prévôt, Fine and coarse PM composition and sources in rural and urban sites in Switzerland: local or regional pollution? Sci. Total Environ. 427–428 (2012) 191–202.

[43] D.P. Gubanova, M.A. Iordanskii, T.M. Kuderina, A.I. Skorokhod, N.F. Elansky, V. M. Minashkin, Elemental composition of aerosols in the near-surface air of moscow: seasonal changes in 2019 and 2020, Atmos. Oceanic Opt 34 (5) (2021) 475–482.
[44] P.R. Unwin, A.G. Güell, G. Zhang, Nanoscale electrochemistry of sp2 carbon materials: from graphite and graphene to carbon nanotubes, Acc. Chem. Res. 49 (9) (2016) 2041–2048.
[45] A. Sadezky, H. Muckenhuber, H. Grothe, R. Niessner, U. Pöschl, Raman microspectroscopy of soot and related carbonaceous materials: spectral analysis and structural information, Carbon 43 (8) (2005) 1731–1742.
[46] I. Chakraborty, S. Banik, R. Biswas, T. Yamamoto, H. Noothalapati, N. Mazumder, Raman spectroscopy for microplastic detection in water sources: a systematic review, Int. J. Environ. Sci. Technol. (2022) 1–14.
[47] C.F. Araujo, M.M. Nolasco, A.M.P. Ribeiro, P.J.A. Ribeiro-Claro, Identification of microplastics using Raman spectroscopy: latest developments and future prospects, Water Res. 142 (2018) 426–440.
[48] E. Schmälzlin, B. Moralejo, M. Rutowska, A. Monreal-Ibero, C. Sandin, N. Tarcea, J. Popp, M.M. Roth, Raman imaging with a fiber-coupled multichannel spectrograph, Sensors (2014) 21968–21980.
[49] R. Dris, J. Gasperi, C. Mirande, C. Mandin, M. Guerrouache, V. Langlois, B. Tassin, A first overview of textile fibers, including microplastics, in indoor and outdoor environments, Environ. Pollut. 221 (2017) 453–458.
[50] K. Liu, X. Wang, N. Wei, Z. Song, D. Li, Accurate quantification and transport estimation of suspended atmospheric microplastics in megacities: implications for human health, Environ. Int. 132 (2019), 105127.
[51] Q. Zhou, C. Tian, Y. Luo, Various forms and deposition fluxes of microplastics identified in the coastal urban atmosphere, Chin. Sci. Bull. 62 (0023–074X) (2017) 3902.
[52] M. Klein, E.K. Fischer, Microplastic abundance in atmospheric deposition within the Metropolitan area of Hamburg, Germany, Sci. Total Environ. 685 (2019) 96–103.
[53] G. Chen, Q. Feng, J. Wang, Mini-review of microplastics in the atmosphere and their risks to humans, Sci. Total Environ. 703 (2020), 135504.
[54] V. Fernández-González, J.M. Andrade, B. Ferreiro, P. López-Mahía, S. Muniategui-Lorenzo, Monitorization of polyamide microplastics weathering using attenuated total reflectance and microreflectance infrared spectrometry, Spectrochim. Acta Mol. Biomol. Spectrosc. 263 (2021), 120162.
[55] M. Di, X. Liu, W. Wang, J. Wang, Manuscript prepared for submission to environmental toxicology and pharmacology pollution in drinking water source areas: microplastics in the Danjiangkou Reservoir, China, Environ. Toxicol. Pharmacol. 65 (2019) 82–89.
[56] S. Allen, D. Allen, V.R. Phoenix, G. Le Roux, P. Durántez Jiménez, A. Simonneau, S. Binet, D. Galop, Atmospheric transport and deposition of microplastics in a remote mountain catchment, Nat. Geosci. 12 (5) (2019) 339–344.
[57] M. González-Pleiter, C. Edo, Á. Aguilera, D. Viúdez-Moreiras, G. Pulido-Reyes, E. González-Toril, S. Osuna, G. de Diego-Castilla, F. Leganés, F. Fernández-Piñas, R. Rosal, Occurrence and transport of microplastics sampled within and above the planetary boundary layer, Sci. Total Environ. 761 (2021), 143213.
[58] M. González-Pleiter, D. Velázquez, C. Edo, O. Carretero, J. Gago, Á. Barón-Sola, L. E. Hernández, I. Yousef, A. Quesada, F. Leganés, R. Rosal, F. Fernández-Piñas, Fibers spreading worldwide: microplastics and other anthropogenic litter in an Arctic freshwater lake, Sci. Total Environ. 722 (2020), 137904.
[59] M. González-Pleiter, C. Edo, D. Velázquez, M.C. Casero-Chamorro, F. Leganés, A. Quesada, F. Fernández-Piñas, R. Rosal, First detection of microplastics in the freshwater of an antarctic specially protected area, Mar. Pollut. Bull. 161 (2020), 111811.
[60] A.R. Aves, L.E. Revell, S. Gaw, H. Ruffell, A. Schuddeboom, N.E. Wotherspoon, M. LaRue, A.J. McDonald, First evidence of microplastics in Antarctic snow, Cryosphere 16 (6) (2022) 2127–2145.
[61] J. Fragão, F. Bessa, V. Otero, A. Barbosa, P. Sobral, C.M. Waluda, H.R. Guímaro, J. C. Xavier, Microplastics and other anthropogenic particles in Antarctica: using penguins as biological samplers, Sci. Total Environ. 788 (2021), 147698.
[62] J.C. Prata, Airborne microplastics: consequences to human health? Environ. Pollut. 234 (2018) 115–126.
[63] C.E. Enyoh, A.W. Verla, E.N. Verla, F.C. Ibe, C.E. Amaobi, Airborne microplastics: a review study on method for analysis, occurrence, movement and risks, Environ. Monit. Assess. 191 (11) (2019) 668.
[64] H.V. Ford, N.H. Jones, A.J. Davies, B.J. Godley, J.R. Jambeck, I.E. Napper, C. C. Suckling, G.J. Williams, L.C. Woodall, H.J. Koldewey, The fundamental links between climate change and marine plastic pollution, Sci. Total Environ. 806 (2022), 150392.